Biology of Reproduction, 2019, 101(1), 188–199
doi:10.1093/biolre/ioz071
Research Article
Advance Access Publication Date: 20 April 2019

Research Article

Intraflagellar transport protein 74 is essential for spermatogenesis and male fertility in mice†

Lin Shi[1,2], Ting Zhou[1,2], Qian Huang[1,2], Shiyang Zhang[1,2], Wei Li[2], Ling Zhang[1], Rex A Hess[3], Gregory J Pazour[4] and Zhibing Zhang[2,5,*]

[1]School of Public Health, Wuhan University of Science and Technology, Wuhan, Hubei, China; [2]Department of Physiology, Wayne State University, Detroit, Michigan, USA; [3]Department of Comparative Biosciences, College of Veterinary Medicine, University of Illinois, Urbana, Illinois, USA; [4]Program in Molecular Medicine, University of Massachusetts Medical School, Worcester, Massachusetts, USA and [5]Department of Obstetrics/Gynecology, Wayne State University, Detroit, Michigan, USA

*__Correspondence:__ Department of Physiology, Department of Obstetrics/Gynecology, Wayne State University, 275 E Hancock Street Detroit, MI 48201, USA. Tel: +313-5770442; E-mail: gn6075@wayne.edu

†__Grant Support:__ This research was supported by NIH grant HD076257, HD090306, and Start-up fund of Wayne State University (to ZZ), GM060992 (to GJP), National Natural Science Foundation of China (81671514, 81571428, 81502792, 81300536, and 81172462), Excellent Youth Science Foundation (2018CFA040) and Youth Foundation (2018CFB114) of Hubei Province, the China Scholarship Council Fund (201808420128), and Special Fund of Wuhan University of Science and Technology for Master Student's short-term studying abroad.
Edited by Dr. Jeremy P. Wang, MD, PhD, University of Pennsylvania
LS, TZ, QH contribute equally in this study.

Received 17 November 2018; Revised 22 March 2019; Accepted 18 April 2019

Abstract

Intraflagellar transport protein 74 (IFT74) is a component of the core intraflagellar transport complex, a bidirectional movement of large particles along the axoneme microtubules for cilia formation. In this study, we investigated its role in sperm flagella formation and discovered that mice deficiency in *Ift74* gene in male germ cells were infertile with low sperm count and immotile sperm. The few developed spermatozoa displayed misshaped heads and short tails. Transmission electron microscopy revealed abnormal flagellar axonemes in the seminiferous tubules where sperm are made. Clusters of unassembled microtubules were present in the spermatids. Testicular expression levels of IFT27, IFT57, IFT81, IFT88, and IFT140 proteins were significantly reduced in the conditional *Ift74* mutant mice, with the exception of IFT20 and IFT25. The levels of outer dense fiber 2 and sperm-associated antigen 16L proteins were also not changed. However, the processed A-Kinase anchor protein, a major component of the fibrous sheath, a unique structure of sperm tail, was significantly reduced. Our study demonstrates that IFT74 is essential for mouse sperm formation, probably through assembly of the core axoneme and fibrous sheath, and suggests that IFT74 may be a potential genetic factor affecting male reproduction in man.

Summary Sentence

IFT74 is essential for mouse spermatogenesis and specifically the sperm flagellum via the assembly of microtubules during formation of the axoneme.

Key words: intraflagellar transport protein 74, spermatogenesis, male fertility, microtubules.

Introduction

Cilia and flagella are microtubule-based organelles that are found on the surface of most eukaryotic cells. They have been adapted for a variety of functions such as cellular motility, directional fluid movement, cellular signaling, and sensory reception [1–3]. The assembly and maintenance of cilia and flagella depend on intraflagellar

transport (IFT), which is a bidirectional movement of large particles along the microtubule-based axoneme between the cell body and the distal tip of cilia/flagella [4, 5]. The IFT machinery is composed of kinesin-2, cytoplasmic dynein, and protein complexes known as A and B [6–8]. The IFT-A complex consists of six subunits (IFT43, IFT121/WDR35, IFT122, IFT139/TTC21B, IFT140, and IFT144/WDR19) and other ancillary proteins, which is powered by dynein 2 to the cilia/flagella tip [9, 10]. The IFT-B complex contains a salt-stable core complex of nine subunits (IFT22, IFT25, IFT27, IFT46, IFT52, IFT70, IFT74, IFT81, and IFT88) and several peripheral components (IFT20, IFT54, IFT57, IFT80, IFT172, and others), which is driven by kinesin-2 to the cell body [4, 6, 7, 10–12]. Defects in the assembly and functions of cilia/flagella, including those in IFT machinery, have been associated with an expanding list of human diseases, including polycystic kidney, obesity, respiratory defects, retinal degeneration, brain, and skeletal malformation, as well as infertility [13–15].

Although the identities of most IFT proteins are known, the specific function of each subunit is poorly understood. As previously reported, the IFT-B complex is much less stable than IFT-A complex in flagellar isolated from *Chlamydomonas* [16, 17]. Within the core subset of IFT-B proteins, IFT25/27, IFT88/52/46, and IFT81/74/72 are considered to interact to form a heterodimer, a ternary complex, and a heterotetramer in a ratio of 2:1:1, respectively [17–19]. It should be noted that the direct interaction of IFT74 and IFT81 through central and C-terminal coiled-coil domains are sufficient to stabilize IFT-B complex [17, 20]. Bhogaraju and colleagues found that the N-termini of both proteins form a tubulin-binding module that enhances the affinity of this interaction. Meanwhile, the N-terminus of IFT74 interacted with the highly acidic C-terminal tails (called as E-hooks) of β-tubulin to enhance the binding affinity of *Homo sapiens* IFT81N bound tubulin by ~18 fold [21]. The tubulin transport is not only crucial for ciliogenesis but is also essential for a balance of cilium assembly and disassembly to maintain cilia length [22, 23]. It is suggested that IFT74/81 complex, not only for ITF81 alone, is required for binding and transport of tubulin to regulate cilium length [21]. In addition, the region near the N-terminus of IFT74 coiled-coil domain 1 is particularly required for the normal association of IFT-A with IFT-B in the cell body of flagella and IFT injection frequency [24]. Thus, IFT74 combined with IFT81 has an important impact on IFT-B complex stabilization, tubulin transport, and cilium formation and length.

It is demonstrated that the mammalian homologue of the IFT74 (referred to as IFT71 in the first report) protein of *Chlamydomonas* is capillary morphogenesis gene-1 product (CMG-1) [25]. Fujino et al. revealed that the mouse *CMG-1* gene was specifically expressed in male germ-line stem cells but not in embryonic stem cells [26]. As previously reported, CMG-1 is localized in the primary cilia and centrosomes, but not in the nucleus of human umbilical vein endothelial cells [25]. However, Ohbayashi and colleagues have recently identified that CMG-1 is broadly distributed in both the cytoplasm and nucleus of GC-2 cells, a mouse premeiotic spermatocyte-derived cell line. Moreover, CMG-1 is required for cell division and niche interactions in the early stages of spermatogenesis in the testis [27].

Even though IFT74 is indispensable for the proliferation of male germ-line stem cells in the mouse testis, the physiological roles of IFT74 in the process of spermatogenesis remain largely unknown. Thus, conditional knockout (KO) strategy was utilized to investigate the potential role of IFT74 in sperm flagella formation and male fertility. With this approach, our laboratory has disrupted mouse *Ift20*, *Ift25,* and *Ift27* genes in male germ cells in mice, and we found that all of them were required for male fertility, spermiogenesis and sperm flagella formation. The study presented here generated the male germ cell-specific *Ift74* KO mice by breeding floxed *Ift74* mice with *Stra8-iCre* mice as previous studies reported [28–30]. We discovered that the conditional *Ift74* KO mice did not show any gross abnormalities, but complete male infertility with dramatically decreased sperm count and aberrant structures of sperm heads and flagella were present. In the conditional *Ift74* KO mice, expression of IFT81 protein, an important IFT74 binding partner, and components of other IFT complex such as IFT27, IFT57, IFT88, and IFT140 proteins were significantly reduced. Our findings suggested that IFT74 is essential for normal mouse spermatogenesis, sperm flagella formation, and male fertility in mice.

Material and methods

Ethics statement

All animal procedures were approved by Wayne State University Institutional Animal Care and Use Program Advisory Committee (Protocol number: IACUC-18-02-0534) in accordance with federal and local regulations regarding the use of nonprimate vertebrates in scientific research.

Generation of *Ift74* condition KO mice

The $Ift74^{Tm1a}$ mice were obtained from the KOMP project at Jackson Laboratory and converted to the $Ift74^{flox}$ allele by FlpE [31]. *Stra8-iCre* mice were purchased from Jackson Laboratory (Stock No:008208). Transgenic mouse line Stra8-cre expresses improved Cre recombinase under the control of a 1.4 Kb promoter region of the germ cell-specific stimulated by retinoic acid gene 8 (Stra8) [32]. To generate the germ cell-specific *Ift74* KO mice, the same breeding strategy used to generate germ cell-specific *Ift20, Ift25,* and *Ift27* KO mice was used [29, 30, 33]. Briefly, 3- to 4-month-old *Stra8-cre* males were crossed with 3- to 4-month-old $Ift74^{flox/flox}$ females to obtain *Stra8-iCre*; $Ift74^{flox/+}$ mice. The 3- to 4-month-old *Stra8-iCre*; $Ift74^{flox/+}$ males were crossed back with 3- to 4-month-old $Ift74^{flox/flox}$ females again, and the *Stra8-iCre;* $Ift74^{flox/flox}$ were considered to be the homozygous KO mice. *Stra8-iCre;* $Ift74^{flox/+}$ mice were used as the controls. The diagram of genomic structure of the floxed and deleted *Ift74* alleles was shown in Figure S1.

Mice were genotyped by PCR using multiplex PCR mix (Bioline, Cat No. BIO25043). To genotype the offspring, genomic DNA was isolated as described previously [34]. The presence of the *Stra8-iCre* allele was evaluated as previous study [32], and *Ift74* genotypes were determined as described as previously. The following primers were used for genotyping: *Stra8-iCre* forward: 5-GTGCAAGCTGAACAA CAGGA-3; *Stra8-iCre* reverse: 5-AGGGACACAGCATTGGAGTC-3, and *Ift74* wild-type primer 1:5-CTGAGTGAAAGTGGAGC-3; primer 2:5-CAAGAAAGCTTGGGTCTAGAT-3; KO primer 3: 5-GAATGCATGTGAAATACATTGTGAA-3; primer 4: 5-GAGAAAAGCAGTAATAGTTCTCATCTCC-3.

Western blot analysis

All tissue samples from 3- to 4-month-old mice were homogenized on ice in lysis buffer [(50 mM Tris–HCl pH 8.0, 170 mM NaCl, 1% NP40, 5 mM EDTA, 1 mM DTT, and protease inhibitors) (Complete mini; Roche diagnostics GmbH)] using Ultra Turrax. Supernatants were collected after being centrifuged at 13000 rpm, for 10 min at 4°C. Protein concentrations were measured using Bio-Rad

Table 1. Antibodies information.

Name	Catalogue number	Purpose	Dilution
Anti-IFT25	15732-1-AP, ProteinTech	Western Blot	1:2000
Anti-IFT74	AS27620e, Antibody Verify	Western Blot, IF	1:2000 for Western Blot; 1:200 for IF
Anti-IFT81	11744-1-AP, ProteinTech	Western Blot	1:1000
β-actin	4967 S, Cell Signaling	Western Blot	1:2000
Anti-IFT20	Dr. Pazour's laboratory	Western Blot	1:2000
Anti-IFT27	Dr. Pazour's laboratory	Western Blot	1:2000
Anti-IFT57	Dr. Pazour's laboratory	Western Blot	1:2000
Anti-IFT88	Dr. Pazour's laboratory	Western Blot	1:2000
Anti-IFT140	Dr. Pazour's laboratory	Western Blot	1:2000
Anti-AKAP4	Dr. George Gerton at University of Pennsylvania	Western Blot	1:4000
Anti-ODF2	12058-1-AP, ProteinTech	Western Blot	1:800
Anti-SPAG16L	Dr. Zhibing Zhang's laboratory	Western Blot	1:1000
Anti-α-tubulin	T9026-2ML, Sigma	IF	1:200
Lectin PNA	L21409, InvitrogenTM	IF	20 μg/ml

DCTM protein assay kit (Bio-Rad) by Lowry assay. Proteins were denatured under 95°C for 10 min, then separated by SDS-PAGE and transferred to polyvinylidene fluoride membranes (Millipore, Billerica, MA, USA). Then the nonspecific sites were blocked in a Tris-buffered saline solution containing 5% nonfat dry milk powder and 0.05% Tween 20 (TBST) for 1 h at room temperature, and the membranes were incubated with indicated primary antibodies (IFT25: 1:2000, Cat No: 15732-1-AP, ProteinTech; IFT74: 1:2000, Cat No: AAS27620e from ANTIBODY VERIFY; IFT81: 1:1000, Cat No: 11744-1-AP, ProteinTech; β-actin: 1:2000, Cat No: 4967 S, Cell Signaling; Antibodies against IFT20, IFT27, IFT57, IFT88, and IFT140 (1:2000) were from Dr Pazour's laboratory [34–36]; A-Kinase anchor protein (AKAP4): 1:4000, from Dr George Gerton at University of Pennsylvania; outer dense fiber 2 (ODF2): 1:800, Cat No: 12058-1-AP, ProteinTech; sperm-associated antigen 16L (SPAG16L): 1:1000, generated by ZZ's laboratory, All of the information were shown in Table 1) at 4°C overnight. After washing three times with TBST, the membranes were incubated with the secondary antibody conjugated with horseradish peroxidase with a dilution of 1:2000 at room temperature for at least 1 h. After washing with TBST twice and a final washing with TBS, the bound antibodies were detected with Super Signal Chemiluminescent Substrate (Pierce, Rockford, IL, USA).

Assessment of fertility and fecundity

To test fertility and fecundity, 6-week-old or 2–3 months old conditional *Ift74* KO and control males were paired with adult wild-type females (3–4 months old). Mating cages typically consisted of one male and one female. Mating behavior was observed, and the females were checked for the presence of vaginal plugs and pregnancy. Once pregnancy was detected, the females were put into separate cages. Breeding tests for each pair lasted for at least three months. The numbers of pregnant mice and offspring from each pregnancy were recorded.

Spermatozoa counting

Sperm were collected from cauda epididymides in warm phosphate-buffered saline (PBS) at 37°C and fixed with 2% formaldehyde for 10 min at room temperature. Sperm were then washed with PBS, suspended in PBS again and counted using a hemocytometer chamber under a light microscope, and sperm number was calculated by standard methods as previously reported [37].

Spermatozoa motility assay

Sperm cells were collected from the cauda epididymides in warm PBS at 37°C. Sperm motility was evaluated using an inverted microscope (Nikon, Tokyo, Japan) on a prewarmed slide with a SANYO (Osaka, Japan) color charge-coupled device, high-resolution camera (VCC-3972) and Pinnacle Studio HD (version 14.0) software. Movies were taken at 15 frames/s. For each sperm sample, 10 fields were selected for analysis. Individual spermatozoa were tracked using NIH Image J (National Institutes of Health, Bethesda, MD) and the plug-in MTrackJ. Sperm motility was calculated as curvilinear velocity (VCL), which is equivalent to the curvilinear distance (DCL) traveled by each individual spermatozoon in one second (VCL = DCL/t).

Histology of tissue sections

Adult mice testes and epididymides were fixed in 4% formaldehyde solution in PBS, paraffin embedded, and 5-μm sections were stained with haematoxylin and eosin using standard procedures. Histology was examined using a BX51 Olympus microscope (Olympus Corp., Melville, NY, Center Valley, PA), and photographs were taken with the ProgRes C14 camera (Jenoptik Laser, Germany).

Isolation of spermatogenic cells and immunofluorescence analysis

Testis from adult mice were dissected in a 15 mL centrifuge tube with 5 mL DMEM containing 0.5 mg/mL collagenase IV and 1.0 μg/mL DNAse I (Sigma-Aldrich) for 30 min at 37°C and shaken gently. Then released spermatogenic cells were washed once with PBS after centrifuging for 5 min at 1000 rpm and 4°C, and the supernatant was discarded. Afterwards, the cells were fixed with 5 mL of 4% paraformaldehyde (PFA) containing 0.1 M sucrose and shaken gently for 15 min at room temperature. After washing three times with PBS, the cell pellet was re-suspended with 2 mL PBS, loaded onto positively charged slides, and stored in a wet box after the sample on slides air-dried. The spermatogenic cells were permeabilized with 0.1% Triton X-100 (Sigma-Aldrich) for 5 min at 37°C, washed with PBS three times and blocked with 10% goat serum for 30 min at 37°C. Then cells were washed with PBS three times and incubated overnight with an anti-IFT74 antibody (1:200). The primary antibodies were the same as those used for western blot analysis, but the dilutions were 10 times higher. Following the secondary antibody incubation, the slides were washed with PBS three times, mounted using VectaMount with 4′,6-diamidino-2-phenylindole (DAPI) (Vector

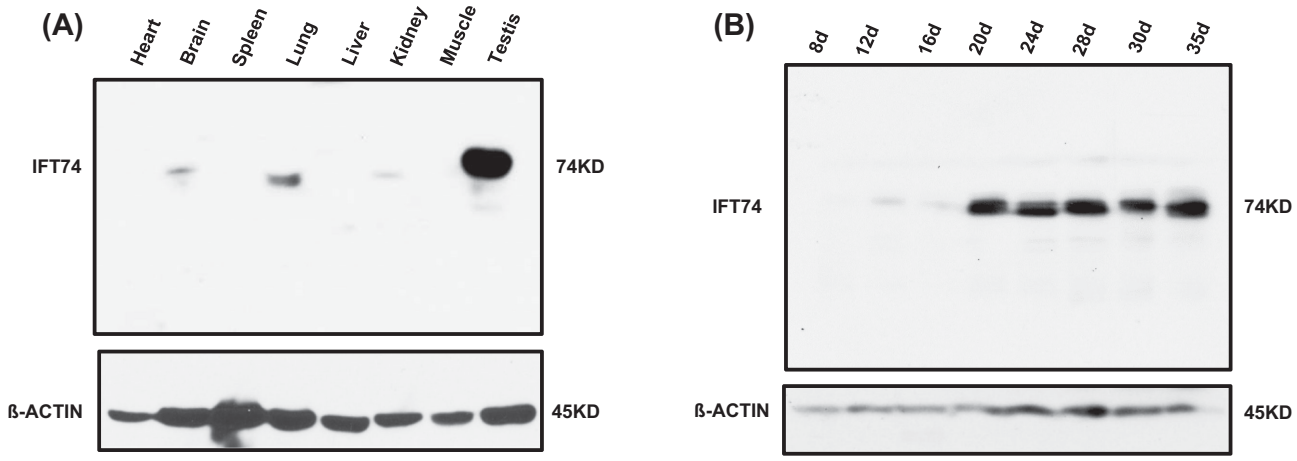

Figure 1. Mouse IFT74 protein is highly expressed in the testis and developmentally regulated during spermatogenesis. (A) Western blot analysis of mouse IFT74 protein, using a high sensitive Femto system. Note that IFT74 is highly expressed in the testis and is also present in the tissues bearing motile and primary cilia, including brain, lung and kidney. (B) IFT74 expression during the first wave of spermatogenesis. Western blot result shows that its expression is significantly increased at day 20 after birth.

Laboratories, Burlingame, CA), and sealed with nail polish. Images were captured by confocal laser-scanning microscopy (Zeiss LSM 700).

Transmission electron microscopy

Testis and epididymal sperm from adult mice were fixed in 3% glutaraldehyde/1% paraformaldehyde/0.1 M sodium cacodylate, pH 7.4 at 4°C overnight and processed for electron microscopy, as in previous reports [30, 38]. Images were taken with a JEOL JEM-1230 transmission electron microscopy (TEM) using a Gatan Orius SC1000 camera.

Scanning electron microscopy

For scanning electron microscopy (SEM) analysis, mouse epididymal sperm were collected and fixed in the same fixative solution as TEM. The samples were processed by standard methods [37] and images were taken with a Zeiss EVO 50 XVP SEM at Microscopy Facility, Department of Anatomy and Neurobiology, Virginia Commonwealth University.

Statistical analysis

All results are given as mean ± standard deviation (SD). Data analysis was performed using SPSS software (version 17.0; SPSS Inc, Chicago, IL). Statistical significance was determined by the Student's t-test. P values < 0.05 were considered to be statistically significant.

Results

IFT74 protein expression and localization in mice

IFT74 protein expression was examined in multiple mouse tissues including heart, brain, spleen, lung, liver, kidney, muscle, and testis by western blot analysis using a highly sensitive Femto system. While the IFT74 protein was present in the other organs containing cilia-bearing cells, such as brain, lung, and kidney, it was highly expressed in the testis (Figure 1A). The level of IFT74 protein was subsequently evaluated in mouse testis at different times during the first wave of spermatogenesis. The IFT74 protein was initially detected at day 12, which exhibited a significant increase in abundance on day 20 and thereafter (Figure 1B).

In addition, immunofluorescence staining was conducted to investigate where the IFT74 protein was localized in isolated germ cells in wild-type mice. Nonspecific staining was not observed in cells where preimmune serum was added (Figure 2Aa). In control mice, the specific IFT74 signal was strongly expressed not only in the vesicles of spermatocytes and round spermatids (Figure 2Ab and c), but appeared also in the acrosome and centrosome regions of elongating spermatids (Figure 2Ad and Bb) and in developing sperm tails (Figure 2Ae). To further confirm the acrosome localization, the cells were double stained with a lectin acrosome marker, peanut agglutinin (PNA), and IFT74 partially colocalized over the acrosomal region (Figure 2Ba, b).

Generation of conditional *Ift74* KO mice

The expression pattern and localization of IFT74 suggested an essential role for the protein in spermatogenesis; therefore, male germ cell-specific conditional KO mice were generated by crossing *Ift74*$^{flox/flox}$ females with *Stra8-iCre* transgenic mice (Figure S1; Figure 2). Testicular IFT74 protein expression in control and conditional *Ift74* mutant mice was determined by western blot analysis and immunofluorescence staining. Western blot results showed that IFT74 protein was absent in the testes of the homozygous mutant mice, whereas it was robustly expressed in all control mice (Figure 3A). Immunofluorescence staining was also conducted in the KO mice. Specific IFT74 signal was observed in the wild type, but not in the KO mice (Figure S3).

Homozygous conditional *Ift74* KO males were infertile, with significantly reduced sperm count and motility

All mutant mice survived to adulthood and did not show gross abnormalities. To evaluate fertility, 3–4 months old controls and homozygous *Ift74* KO males were bred to 3- to 4-month-old wild-type females for at least 2 months. All six control males were fertility and sired normal size litters. However, all six *Ift74* mutant males were infertile and did not produce any litters during the breeding period

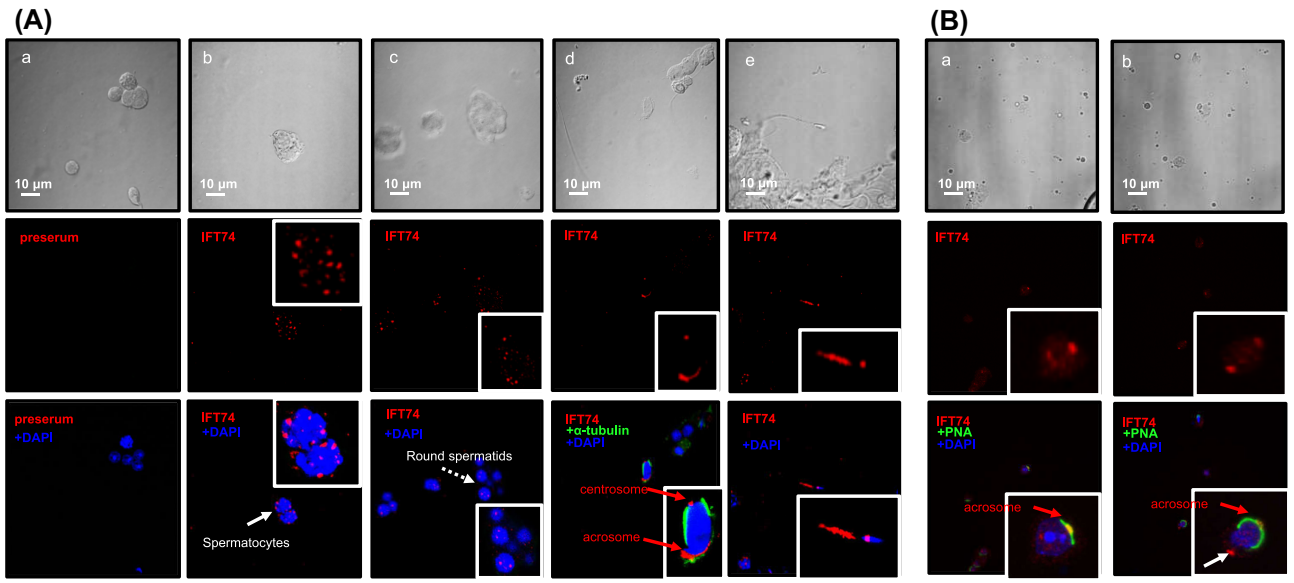

Figure 2. Localization of IFT74 in male germ cells. (A) Immunofluorescence staining of IFT74 in germ cells of wild-type mice. The top row shows the germ cells with phase contrast microscopy. No specific signal was detected in the negative control using preimmune serum (a). It is present as vesicles in spermatocytes (arrow and inset in b) and round spermatids (dashed arrow and inset in c). It appears to be present in the acrosome and centrosome of elongating spermatid (d), and developing tail (inset in e). (B) The cells were double stained with a lectin acrosome marker, peanut agglutinin (PNA). IFT74 was colocalized with PNA. In addition, it was also present as a dot at the opposite region of the acrosome (white arrow), presumably the centriole.

(Table 2). To investigate the mechanisms that underline the infertility, sperm number and motility were examined. The control mice had a normal sperm count and motility (Figure 3B–D; Movie S1A). Sperm count was reduced in the conditional *Ift74* KO mice (Figure 3B) and there was a significant reduction in the percentage of motile sperm (Figure 3C). Sperm motility was also dramatically reduced in the conditional *Ift74* KO mice (Figure 3D; Movie S1B).

Abnormal epididymal sperm in the conditional *Ift74* KO mice

To further identify sperm changes associated with the infertility phenotype, morphology of cauda epididymal sperm was analyzed by SEM (Figure 4). Sperm from control mice had well-shaped heads and long, smooth tails (Figure 4a). However, in the conditional *Ift74* KO mice, few sperm could be collected from the cauda epididymides and all evaluated were abnormal. A variety of abnormalities were observed in the mutant sperm, including very short tails and mostly abnormally shaped heads, with only rare sperm having a normal appearing head (Figure 4b–f).

Abnormal spermiogenesis in the conditional *Ift74* KO mice

To analyze changes in spermatogenesis that may contribute to low sperm counts and abnormal sperm morphology, histology of testes in control and the conditional *Ift74* KO mice were examined and stages of the seminiferous tubules were determined [39] (Figure 5A; Figure S4A). There was no significant difference in testis/body weights between controls and mutant mice (Table 2). In control mice, testes exhibited an integrated and normal spermiogenesis (Figure 5Aa). However, testes of the conditional *Ift74* KO mice showed a failure of spermiation in stage VIII, with abnormal step 16 spermatids (Ab16) being phagocytized, although in the same tubule step 8 round spermatids and pachytene spermatocytes (P) appeared normal. Also, normal residual bodies were not formed. Instead, small pieces of germ cell cytoplasm (Cy) were retained at the luminal border (Figure 5Ab) or sloughed into the lumen, as found in the epididymis (Figure 5Bb). In mutant stage XI, abnormal step 11 spermatids (Ab 11) were observed with misshaped heads and the absence of sperm tails (Figure 5Ac). Mutant stage I tubules showed normal round spermatids, but there was abnormal step 13 elongating spermatids (Ab13) lacking tails. Excess cytoplasm (Cy) of the elongating spermatids appeared to be sloughed into the lumen (Figure 5Ad).

Abnormal spermatogenesis in the conditional *Ift74* KO mice was also manifested by the presence of abnormal luminal contents in the cauda epididymis (Figure 5B; Figure S4B). In control mice, compacted epididymal sperm, with aligned normal heads and tails, filled the lumen (Figure 5Ba; Figure S4B, upper panels). However, the epididymal lumen of conditional *Ift74* KO mice contained massive amounts of large abnormal cytoplasmic bodies, residual bodies, sloughed round cells, and abnormal spermatids with short or absent tails (Figure 5Bb; Figure S4B, lower panels).

Ultrastructure of seminiferous tubules was determined by TEM in the control and conditional *Ift74* KO mice (Figure 6; Figure S5). In control mice, a large number of axonemes were present in the lumen (Figure 6a). However, in the seminiferous tubules of the conditional *Ift74* KO mice, a variety of axonemal abnormalities were discovered. Spermatid abnormalities included the following: a complete absence of the axoneme (Figure 6b; Figure S5a), disorganized microtubules (Figure 6c; Figure S5b, f, g), clusters of microtubules (Figure 6d), and abnormally formed axonemes without the central microtubules (Figure 6e). Although the acrosome of spermatids appeared to be normal (Figure 6h), there were some abnormally shaped heads on elongating spermatids (Figure 6f and h; Figure S5c–e).

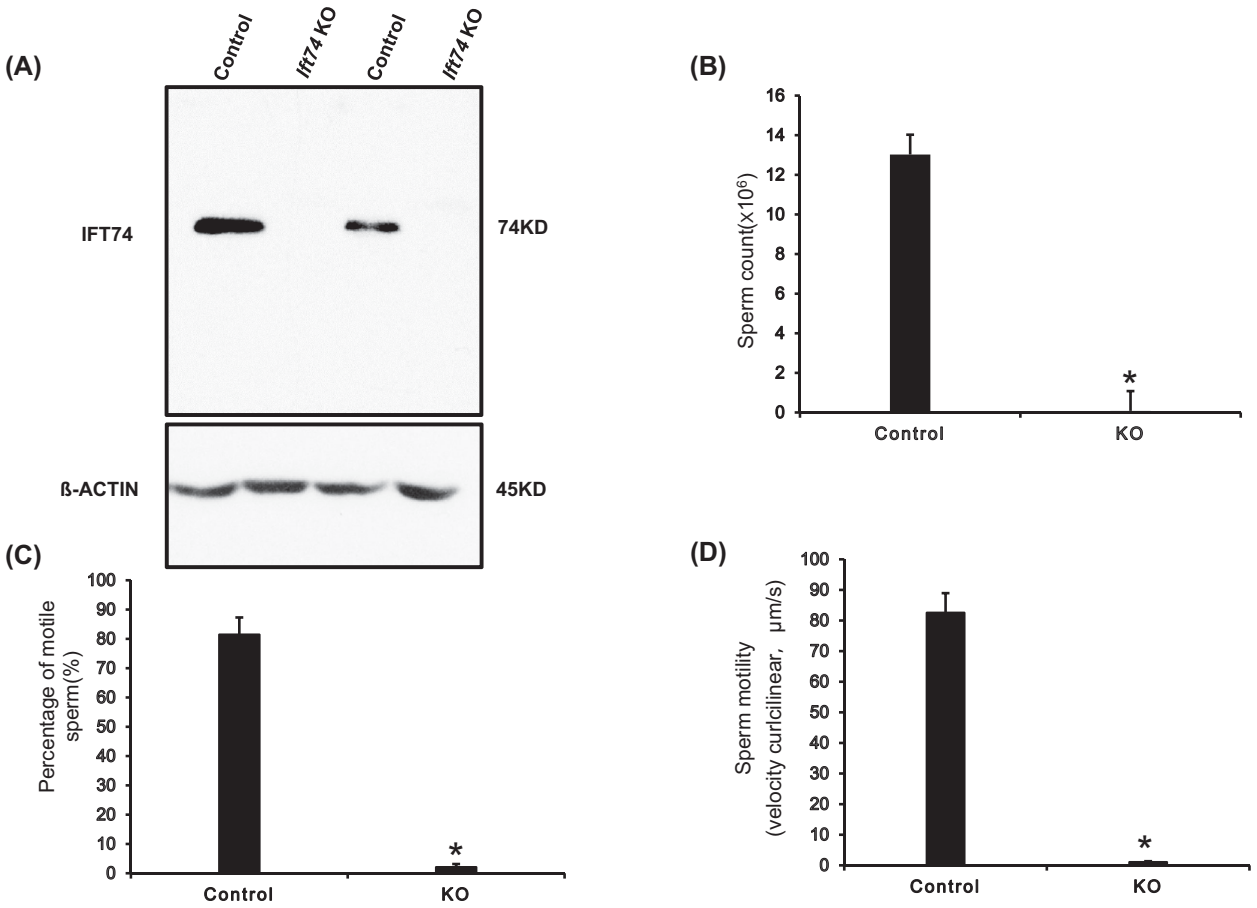

Figure 3. Significant reduction in sperm numbers and motility in the conditional *Ift74* KO mice. (A) Western blot analysis of testicular IFT74 protein expression in control and conditional *Ift74* KO mice. Note that IFT74 protein was missing in the conditional KO mice. Epididymal sperm were collected and physiologic parameters were compared between the control and conditional *Ift74* KO mice. In the conditional *Ift74* KO mice, there are significant reductions in sperm count (B), percentage of motile sperm (C), and sperm motility (D). Data are expressed as the Means ± SD (n = 4). $^{*}P < 0.05$ compared with the control mice.

Table 2. Homozygous *Ift74* KO males were infertile.

Genotype	Fertility	Litter size	Testis/body weight (mg/g)
Control	6/6	7 ± 2	9.47 ± 0.68 (n = 6)
KO	0/6	0	8.31 ± 0.52 (n = 6)

To test fertility, 3- to 4-month-old control and conditional *Ift74* KO mice were bred to 3- to 4-month-old wild-type females for at least 2 months. Litter size was recorded for each mating. Data are expressed as Mean ± SD.

IFT74 regulates cellular levels of other IFT proteins and some flagellar proteins

To understand how the loss of IFT74 affects other IFT and flagellar proteins, we determined the levels of selective IFT and flagellar proteins in the testis of control and conditional *Ift74* KO mice by western blot. The protein levels of components of the IFT-B complex, such as IFT27, IFT57, IFT81, IFT88 and IFT140 were significantly decreased in the conditional *Ift74* KO mice; however, the IFT20 and IFT25 proteins, two additional components of the IFT-B complex, did not differ from those expressed in control mice (Figure 7A). Moreover, IFT74 did not affect testicular expression levels of ODF2, a major component of the sperm tail outer dense fibers, and an axonemal central apparatus protein, SPAG16L. However, AKAP4, a processed form of the major component of the fibrous sheath, was significantly reduced in the KO mice (Figure 7B).

Discussion

In this study, we first characterized the expression pattern of IFT74 in male germ cells, and then examined the reproductive phenotype of conditional *Ift74* KO mice. IFT74 was found to be highly expressed during spermiogenesis, suggesting a specific role in the morphological changes that germ cell undergo during differentiation, particularly formation of the sperm flagellum. This function is consistent with the conserved role of IFT in cilia formation and is further supported by its localization. During spermatogenesis, IFT74 is associated with vesicles in spermatocytes and round spermatids, with the acrosome and centrosome of elongating spermatids, and in the developing sperm tails. The acrosome is a unique membranous organelle formed only in male germ cells [40]. It was initially thought to be a modified lysosome [41], but subsequent studies established that the acrosome is a Golgi-derived secretory vesicle [42]. Berruti and Paiardi recently revisited the notion that the acrosome is a novel lysosome-related organelle (LRO) [40]. LROs have functional and dynamic stages of maturation as indicated by the involvement of many proteins critical for vesicle fusion and transport. IFT74 does not appear to be present in the Golgi bodies.

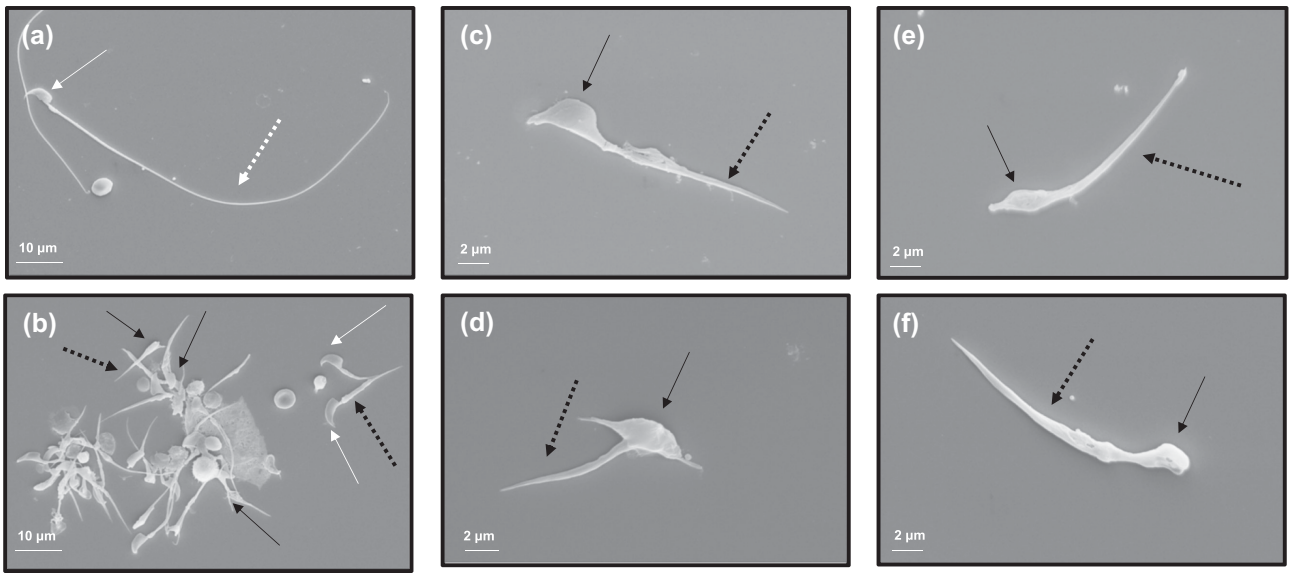

Figure 4. Abnormal epididymal sperm in the conditional *Ift74* KO mice. Examination of epididymal sperm by SEM. (a) Representative image of epididymis sperm with normal morphology from a control mouse. The sperm has a normally shaped head (white arrow) and a long, smooth tail (white dashed arrow). (b–d) Representative images of epididymal sperm from a conditional *Ift74* KO mice. All sperm have short tails (black dashed arrow) and most have grossly abnormal heads (black arrow). Panels c to f show sperm with both abnormal heads (black arrow) and short abnormal tails (black dashed arrow).

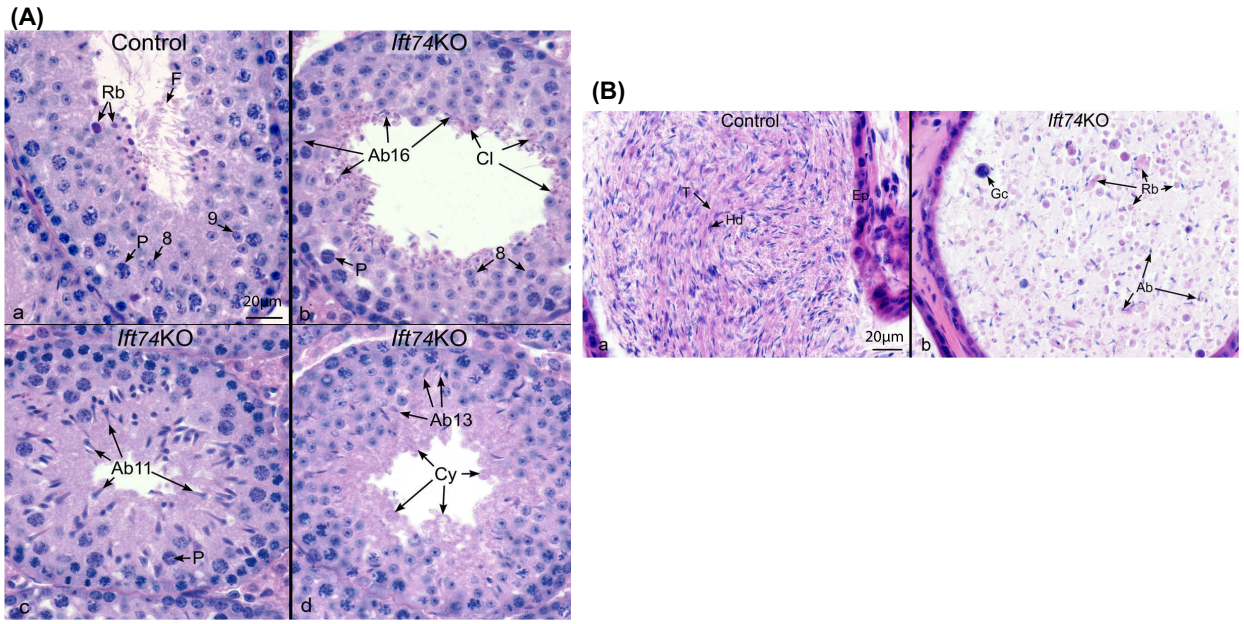

Figure 5. Abnormal spermiogenesis in the conditional *Ift74* KO mice (HE, ×40). (A) Testis histology from control and the conditional *Ift74* KO mice showing cross-sections of seminiferous tubules. Bar = 20 μm. (a) Control seminiferous tubule Stage VIII-IX, showing steps 8 and 9 round spermatids, flagella (F) of sperm being released into the lumen and residual bodies (Rb) of germ cell cytoplasm being phagocytized by Sertoli cells. P, pachytene spermatocyte. (b) The conditional *Ift74* KO seminiferous tubule in Stage VIII, showing normal step 8 round spermatids and pachytene spermatocytes (P). Abnormal step 16 spermatids (Ab16) are seen being phagocytized and failing to spermiation. Residual bodies are not forming but small pieces of germ cell cytoplasm (Cy) are retained at the luminal border. (c) The conditional *Ift74* KO Stage XI with abnormal step 11 spermatids (Ab11) with abnormally shaped heads and absence of tails. P, pachytene spermatocyte. (d) The conditional *Ift74* KO tubule showing normal round spermatids but abnormal step 13 elongating spermatids (Ab13) that are lacking tails. Excess cytoplasm (Cy) of the elongating spermatids appears to be sloughed into the lumen. (B) Cauda epididymis from control and the conditional *Ift74* KO mice. Bar = 20 μm. (a) Control epididymis showing an epithelium (Ep) lining the lumen that is filled with normal sperm aligned with their heads (Hd) and tails (T). (b) The conditional *Ift74* KO epididymis showing a lumen filled with numerous, large cytoplasmic bodies that are likely residual bodies (Rb) and sperm with abnormal heads (Ab) and short or absent tails. Gc, sloughed round spermatid.

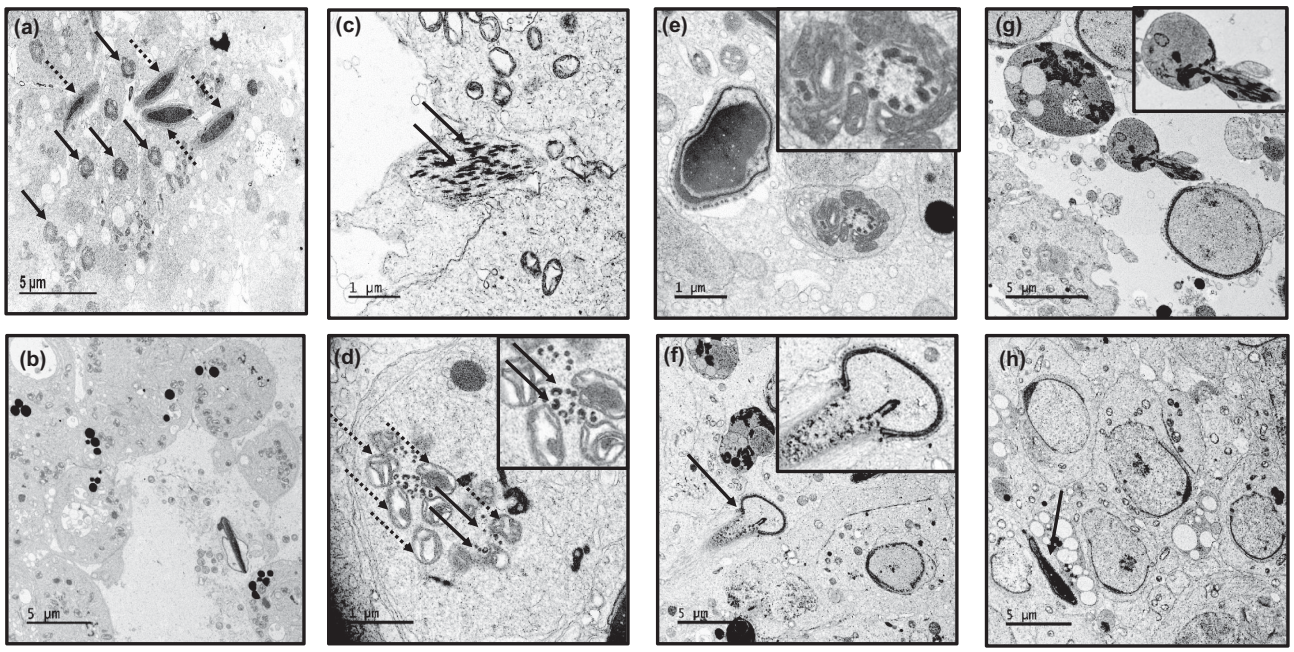

Figure 6. Ultrastructural changes in the testis of conditional *Ift74* KO mice. Testicular ultrastructural was analyzed in the conditional *Ift74* KO mice. (a) Control mouse TEM image. The arrows in "a" point to the axoneme/tail of sperm, and dashed arrows point to the well-formed heads. Numerous axonemes of sperm tails are seen. (b–h) *Ift74* mutant mouse testis. "b" shows the lumen area with the absence of normal axonemal structures. The arrows in (c) points to disorganized microtubules; the inset in "d" shows clusters of microtubules (arrows) and mitochondria (dashed arrows) without a core axoneme structure; the inset in "e" shows an abnormally formed axoneme without the central microtubules; the inset in "f" shows an abnormally formed elongating spermatid; "g" shows sloughed residual bodies and abnormal spermatids; the inset in "g" shows an abnormal spermatid. The developing acrosome appears to be normal (h). The arrows in "f" and "h" point to abnormal spermatid heads.

Association with the cytoplasmic vesicles in spermatocytes and round spermatids strongly suggests that the protein is involved in vesicle fusion within the acrosome. However, given that the acrosome formation was not affected in the *Ift74* mutant mice, IFT74 is not the key factor to control acrosome biogenesis, but only carrying "unidentified materials" to the acrosome. The centrosome is a major organizer of microtubules, has important functions in regulating cell shape, polarity, cilia formation, and intracellular transport as well as the position of cellular structures [43]. During ciliogenesis, centrioles can also be modified to form basal bodies, which template the formation of cilia [44]. Thus, IFT74 localization in the centrosome supports the potential role of the protein in transporting cargo proteins for sperm flagella formation.

This potential role is consistent with previous studies [45] showing that IFT74 localizes in the proximal region of developing flagella and base of the mature flagellum in wild-type cells [46], which suggests that IFT74 may be involved in carrying cargo proteins responsible for formation of the sperm flagellum. This hypothesis is strongly supported by data obtained in the conditional *Ift74* KO mice. The homozygous males were infertile due to low sperm count and significantly reduced sperm motility. Abnormalities in sperm morphology were also observed, such as round and distorted heads, short tails, and a great diversity of axonemal and microtubular abnormalities in spermatids from the conditional *Ift74* KO mice. Given that a major ultrastructural observation was the lack of microtubule assembly in spermatids, it is likely that one of IFT74's major functions in testis is the transport of β-tubulin for microtubule assembly during formation of the axoneme in differentiating spermatids.

It has been shown that IFT74 is expressed in spermatogonia and, most abundantly, in premeiotic spermatocytes [27]. It is essential for the expression of *cyclin-D2* in the mouse premeiotic spermatocyte-derived GC-2 cell line [26]. Furthermore, siRNA-mediated knockdown of *Ift74* in GC-2 cells resulted in a significant reduction of protein levels of cell-adhesion molecules such as E-cadherin protein that is required for the initial cell division of spermatogonial stem cells [47]. These findings from in vitro studies were not consistent with our in vivo observations from the conditional *Ift74* KO mice. Even though IFT74 protein is first detected on day 12 after birth in control testes, the KO mice phenotype was not observed until the spermiogenesis phase. One possibility is that Cre activity is low in mitosis and meiosis phases driven by *Stra8* promoter [32]. To better understand the role of IFT74 in mitosis and meiotic development of male germ cells, a different transgenic Cre mouse model should be used in which Cre activity is higher at these phases.

The function of IFT74 seems to be conserved between *Chlamydomonas reinhardtii* and mouse. In *Chlamydomonas reinhardtii Ift74* null mutant cells had no cilia or only short cilia [24]. In the conditional *Ift74* KO mice, a consistent observation was the lack of axoneme formation in seminiferous tubules, and when occasionally present the sperm had very short tails. Moreover, the accumulation of disorganized microtubules in mutant spermatid cytoplasm suggests a failure to incorporate tubulin into the flagellum, which would be consistent with the known function of IFT74 as a tubulin carrier. In *Chlamydomonas,* many *Ift74* mutant flagella showed no IFT movements and severe defects of IFT injection [24, 48, 49]. Even though there is limited visibility of IFT protein in the flagellum, IFT frequency and retrograde velocity are both dramatically reduced in the mutant compare with wild-type cells, suggesting that IFT74 could be another master regulator controlling sperm formation by modulating axoneme and microtubule assembly.

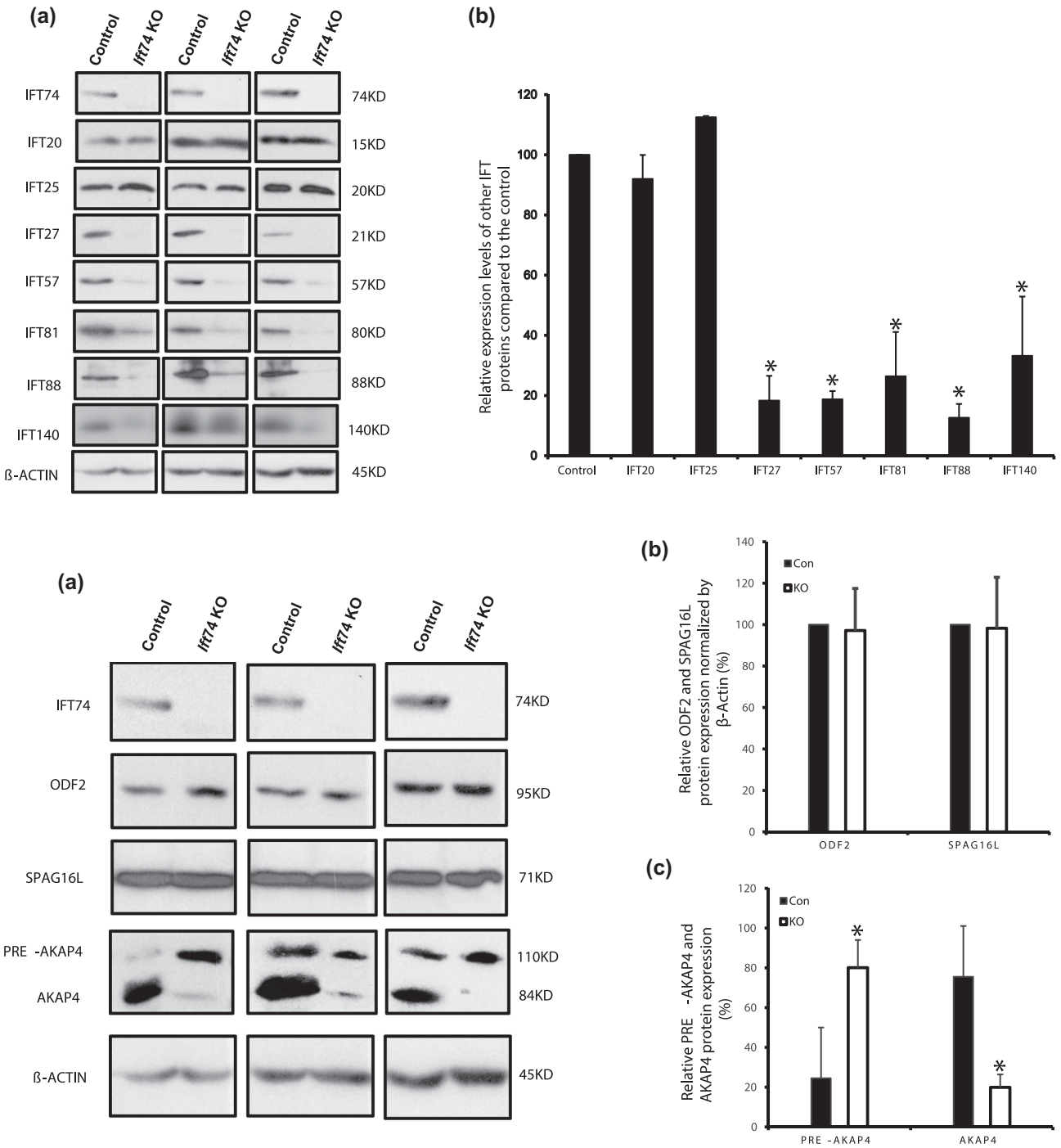

Figure 7. IFT74 regulates expression levels of some IFT and flagellar proteins. (A) Examination of selective IFT protein expression levels in the control and conditional *Ift74* KO mice by western blot. Compared to the controls, the expression levels of IFT27, IFT57, IFT81, IFT88, and IFT140, but not IFT20 and IFT25 are reduced in the conditional *Ift74* KO mice. (a) Representative western blot result; (b) quantitative analysis of selective IFT protein expression. (B) Examination of testicular expression levels of ODF2, a component of sperm tail outer dense fibers, AKAP4, a major component of fibrous sheath, and SPAG16L, a component of axonemal central apparatus protein in the control and conditional *Ift74* KO mice. There was no difference in ODF2 and SPAG16L expression. However, the processed AKAP4 was significantly reduced in the conditional *Ift74* KO mice. β-ACTIN was used as controls. (a) Representative western blot result; (b) quantitative analysis of ODF2 and SPAG16L; (c) quantitative analysis of AKAP4. Data are expressed as means $\pm$ SD (n = 3). $^*P < 0.05$ compared with the control mice.

The concept that IFT74 may serve as a master regulator of axoneme assembly is supported by Brown and colleagues' study that IFT74 is required to stabilize IFT-B and flagella assembly [24]. It has been shown that IFT74 and IFT81 interact directly through not only central and C-terminal coiled-coil domains, but also the N-termini of both proteins to enhance the IFT-B complex stability [17, 21]. Defect in IFT74 function is likely to affect the interactions of these proteins and the stability of IFT81 formed IFT-B complex. The levels of both core IFT81 and IFT57 proteins are lower in *Chlamydomonas reinhardtii Ift74* mutants than that in wild-type cells [24]. This function seems to be conserved also in mouse.

Testicular expression levels of most IFT components examined, including IFT27, IFT57, IFT81, and IFT88, IFT140 were reduced in the conditional *Ift74* KO mice, suggesting that IFT74 is a core IFT component that has a significant influence in the stability and functions of other IFTs during spermiogenesis. These proteins might be gradually degraded when IFT complex is unable to assemble without expression of the *Ift74* gene. This differs from several other conditional *Ift* KO mice. In conditional *Ift25*, *Ift27,* and *Ift140* KO mice, expression levels of most IFT proteins, particularly IFT74, were not changed [29, 30]. It has been demonstrated that both peripheral proteins (IFT20 and IFT25) are localized outside of the core IFT-B subcomplex, and their behaviors are possibly different from other IFT-B proteins [18, 50–52], which would explain why there was no change in IFT20 and IFT25 expression levels in the *Ift74* KO mice. In *Ift25* mutant mice, the IFT20 protein level was significantly reduced, but IFT74 protein was still present similar to that of wild-type mice [29]. It appears that IFT20 and IFT25 form a subcomplex that does not include IFT74 in male germ cells. It has been reported that IFT25 dimerizes with IFT27 [53]. Therefore, we were not surprised to discover that the testicular IFT25 levels were reduced in the conditional *Ift27* mutant mice [30]. Given that testicular IFT27 is missing in the *Ift25* mutant mice, it is possible that all IFT27 associates with IFT25 in male germ cells, but some IFT25 does not associate with IFT27. A reduction in the IFT27 level was not sufficient to reduce the IFT25 level. The IFT25 level was maintained unchanged by an unknown compensatory mechanism. However, when IFT27 is missing, the compensatory mechanism appears not to be sufficient to maintain IFT25 levels. This would help to explain why disruption of *Ift74* only causes the reduction of IFT27, but not IFT25.

Testicular ODF2 and SPAG16L protein levels were not changed in the conditional *Ift74* KO mice. In the conditional *Ift20* KO mice, ODF2 and SPAG16L, two sperm flagella proteins, fail to be incorporated into sperm tails [33]; thus, the potential role of IFT74 in the localization of these proteins remains to be determined. It is possible that loss of *Ift74* in male germ cells only causes an abnormal distribution of these proteins, but does not alter their levels. Interestingly, the expression pattern of a sperm fibrous sheath protein, AKAP4 was changed in the absence of IFT74. *Akap4* gene is translated as a full length 110 kDa precursor (pro-AKAP4). The pro-AKAP4 should be transported from cytoplasm to the fibrous sheath assemble site, presumably by IFT. A 26 kDa peptide is processed out at the fibrous sheath assemble site, and the 84 kDa AKAP4 is incorporated into sperm fibrous sheath [54, 55]. In the wild-type mice testis, the AKAP4 seems to be the predominant form, and the pro-AKAP4 level is significantly less than AKAP4. However, in the *Ift74* KO mice, pro-AKAP4 became the predominant form. The reason might be that the pro-AKAP4 is not transported to the fibrous sheath assemble site due to disrupted IFT, and the precursor is not processed. It is also possible that there was a reduction in the number of elongated spermatids in the conditional *Ift74* mice, which could also explain the reduction of AKAP4 and accumulation of pro-AKAP4. However, there are some similarities between the present study and the *Akap4* knock-out mice, which have abnormally developed fibrous sheaths, poor sperm motility and the males are infertile [56].

In conclusion, we explored the role of IFT74 in mouse sperm development and male fertility and the findings support that IFT74 is essential for mouse spermatogenesis and specifically the sperm flagellum via the assembly of microtubules during formation of the axoneme. By analyzing the expression of other IFT components and sperm flagella proteins, we have concluded that IFT74 may function as a core component of the IFT-B complex to modulate its stability.

Supplementary data

Supplementary data are available at *BIOLRE* online.

Figure S1. Diagram of mouse genomic structure of the floxed and deleted *Ift74* alleles. Note that the two LoxP sites are flanking exon 3.

Figure S2. Representative PCR results showing mice with different genotypes. Upper panel: primer set to analyze *Ift74* genotyping; lower panel: primer set to detect *Cre*.

Figure S3. IFT74 signal is missing in the male germ cells isolated from the conditional *Ift74* KO mice. Note that strong IFT74 signal was observed in the germ cells isolated from a control mouse (upper panel); however, no specific signal was detected in the germ cells isolated from the conditional *Ift74* KO mice (lower panel).

Figure S4. Low magnification images of histology of testis and epididymis of adult control and conditional *Ift74* mutant mice. (A) Testis sections. Note that seminiferous tubules in the control mice (upper) contain normally developed germ cells, and sperm were found in the lumen (arrow). In the mutant mice (lower), the seminiferous tubules were almost empty in the lumen. (B) Epididymal sections. The epididymal lumens of a control mouse (upper) are filled with well-developed sperm. In *Ift74* mutant (lower), the cauda epididymal lumen contains sloughed spermatids, numerous detached sperm heads and abnormal tails and other cellular debris.

Figure S5. Additional ultrastructural changes in the testis of conditional *Ift74* KO mice. (a) The lumen of seminiferous tubule had degenerated cells and axoneme structure were hardly seen. (b) disorganized microtubules (arrows) in the cytoplasm of an abnormally developed spermatid; (c–e) abnormally condensed chromatin (arrows): abnormally condensed chromatin (arrow), misorganized mitochondria (dashed arrows); (f and g) disorganized microtubules (arrows); (h) an abnormally localized axoneme (arrow), representing an abnormal spermatid that is being phagocyted by a Sertoli cell.

Movie S1. Examples of sperm motility patterns from the control mice and the conditional *Ift74* mutant mice. The movies are short segments of freshly isolated, noncapacitated sperm from a control (A) and the conditional *Ift74* mutant mice (B). All segments were recorded with a DAGE-MTI DC-330 3CCD camera and a Canon Optura 40 digital camcorder. Segments were assembled into the video using iMovie HD on a Dual 1GHz 414 PowerPC Processor G4 Apple Macintosh computer.

Movie S1A. A representative movie from a control mouse. Note that most sperm are motile and display vigorous flagellar activity and progressive, long-track forward movement.

Movie S1B. A representative movie from a conditional *Ift74* mutant mouse. Note that there are fewer sperm compared to the control mice, with the same dilution, and all sperm are immotile. A large number of degenerated cells are also present.

Conflicts of Interest: The authors have declared that no conflict of interest exists.

References

1. Wheatley DN. Primary cilia in normal and pathological tissues. *Pathobiology* 1995; **63**(4):222–238.
2. Bray D. *Cell Movements: From Molecules to Motility*, New York, NY: Garland Publishing; 2001:225–241.
3. Praetorius HA, Spring KR. A physiological view of the primary cilium. *Annu Rev Physiol* 2005; **67**(1):515–529.
4. Kozminski KG, Johnson KA, Forscher P, Rosenbaum JL. A motility in the eukaryotic flagellum unrelated to flagellar beating. *Proc Natl Acad Sci* 1993; **90**(12):5519–5523.
5. Kozminski KG, Beech PL, Rosenbaum JL. The Chlamydomonas kinesin-like protein FLA10 is involved in motility associated with the flagellar membrane. *J Cell Biol* 1995; **131**(6):1517–1527.
6. Cole DG, Diener DR, Himelblau AL, Beech PL, Fuster JC, Rosenbaum JL. Chlamydomonas kinesin-II-dependent intraflagellar transport (IFT): IFT particles contain proteins required for ciliary assembly in Caenorhabditis elegans sensory neurons. *J Cell Biol* 1998; **141**(4):993–1008.
7. Pazour GJ, Dickert BL, Witman GB. The DHC1b (DHC2) isoform of cytoplasmic dynein is required for flagellar assembly. *J Cell Biol* 1999; **144**(3):473–481.
8. Piperno G, Mead K. Transport of a novel complex in the cytoplasmic matrix of Chlamydomonas flagella. *Proc Natl Acad Sci* 1997; **94**(9):4457–4462.
9. Ishikawa H, Marshall WF. Ciliogenesis: building the cell's antenna. *Nat Rev Mol Cell Biol* 2011; **12**(4):222–234.
10. Taschner M, Bhogaraju S, Lorentzen E. Architecture and function of IFT complex proteins in ciliogenesis. *Differentiation* 2012; **83**(2):S12–S22.
11. Porter ME, Bower R, Knott JA, Byrd P, Dentler W. Cytoplasmic dynein heavy chain 1b is required for flagellar assembly in Chlamydomonas. *Mol Biol Cell* 1999; **10**(3):693–712.
12. Taschner M, Lorentzen E. The Intraflagellar Transport Machinery. *Cold Spring Harb Perspect Biol* 2016; **8**(10):a028092.
13. Hildebrandt F, Benzing T, Katsanis N. Ciliopathies. *N Engl J Med* 2011; **364**(16):1533–1543.
14. Brown JM, Witman GB. Cilia and diseases. *Bioscience* 2014; **64**(12):1126–1137.
15. Fliegauf M, Benzing T, Omran H. When cilia go bad: cilia defects and ciliopathies. *Nat Rev Mol Cell Biol* 2007; **8**(11):880–893.
16. Signor D, Wedaman KP, Rose LS, Scholey JM. Two heteromeric kinesin complexes in chemosensory neurons and sensory cilia of Caenorhabditis elegans. *Mol Biol Cell* 1999; **10**(2):345–360.
17. Lucker BF, Behal RH, Qin H, Siron LC, Taggart WD, Rosenbaum JL, Cole DG. Characterization of the intraflagellar transport complex B core: direct interaction of the IFT81 and IFT74/72 subunits. *J Biol Chem* 2005; **280**(30):27688–27696.
18. Wang Z, Fan ZC, Williamson SM, Qin H. Intraflagellar transport (IFT) protein IFT25 is a phosphoprotein component of IFT complex B and physically interacts with IFT27 in Chlamydomonas. *PLoS One* 2009; **4**(5):e5384.
19. Lucker BF, Miller MS, Dziedzic SA, Blackmarr PT, Cole DG. Direct interactions of intraflagellar transport complex B proteins IFT88, IFT52, and IFT46. *J Biol Chem* 2010; **285**(28):21508–21518.
20. Taschner M, Bhogaraju S, Vetter M, Morawetz M, Lorentzen E. Biochemical mapping of interactions within the intraflagellar transport (IFT) B core complex: IFT52 binds directly to four other IFT-B subunits. *J Biol Chem* 2011; **286**(30):26344–26352.
21. Bhogaraju S, Cajanek L, Fort C et al. Molecular basis of tubulin transport within the cilium by IFT74 and IFT81. *Science* 2013; **341**(6149): 1009–1012.
22. Marshall WF, Rosenbaum JL. Intraflagellar transport balances continuous turnover of outer doublet microtubules: implications for flagellar length control. *J Cell Biol* 2001; **155**(3):405–414.
23. Sharma N, Kosan ZA, Stallworth JE, Berbari NF, Yoder BK. Soluble levels of cytosolic tubulin regulate ciliary length control. *Mol Biol Cell* 2011; **22**(6):806–816.
24. Brown JM, Cochran DA, Craige B, Kubo T, Witman GB. Assembly of IFT trains at the ciliary base depends on IFT74. *Curr Biol* 2015; **25**(12):1583–1593.
25. Iomini C, Tejada K, Mo W, Vaananen H, Piperno G. Primary cilia of human endothelial cells disassemble under laminar shear stress. *J Cell Biol* 2004; **164**(6):811–817.
26. Fujino RS, Ishikawa Y, Tanaka K, Kanatsu-Shinohara M, Tamura K, Kogo H, Shinohara T, Hara T. Capillary morphogenesis gene (CMG)-1 is among the genes differentially expressed in mouse male germ line stem cells and embryonic stem cells. *Mol Reprod Dev* 2006; **73**(8): 955–966.
27. Ichiro Ohbayashi K, Tanaka K, Kitajima K, Tamura K, Hara T. Novel role for the intraflagellar transport protein CMG-1 in regulating the transcription of cyclin-D2, E-cadherin and integrin-alpha family genes in mouse spermatocyte-derived cells. *Genes Cells* 2010; **15**(7):699–710.
28. Jonassen JA, San Agustin J, Follit JA, Pazour GJ. Deletion of IFT20 in the mouse kidney causes misorientation of the mitotic spindle and cystic kidney disease. *J Cell Biol* 2008; **183**(3):377–384.
29. Liu H, Li W, Zhang Y, Zhang Z, Shang X, Zhang L, Zhang S, Li Y, Somoza AV, Delpi B, Gerton GL, Foster JA et al. IFT25, an intraflagellar transporter protein dispensable for ciliogenesis in somatic cells, is essential for sperm flagella formation. *Biol Reprod* 2017; **96**(5):993–1006.
30. Zhang Y, Liu H, Li W, Zhang Z, Shang X, Zhang D, Li Y, Zhang S, Liu J, Hess RA, Pazour GJ, Zhang Z. Intraflagellar transporter protein (IFT27), an IFT25 binding partner, is essential for male fertility and spermiogenesis in mice. *Dev Biol* 2017; **432**(1):125–139.
31. Farley FW, Soriano P, Steffen LS, Dymecki SM. Widespread recombinase expression using FLPeR (flipper) mice. *Genesis* 2000; **28**(3-4):106–110.
32. Sadate-Ngatchou PI, Payne CJ, Dearth AT, Braun RE. Cre recombinase activity specific to postnatal, premeiotic male germ cells in transgenic mice. *Genesis* 2008; **46**(12):738–742.
33. Zhang Z, Li W, Zhang Y, Zhang L, Teves ME, Liu H, Strauss JF, 3rd, Pazour GJ, Foster JA, Hess RA, Zhang Z. Intraflagellar transport protein IFT20 is essential for male fertility and spermiogenesis in mice. *Mol Biol Cell* 2016; **27**(23):3705–3716.
34. Keady BT, Samtani R, Tobita K, Tsuchya M, San Agustin JT, Follit JA, Jonassen JA, Subramanian R, Lo CW, Pazour GJ. IFT25 links the signal-dependent movement of Hedgehog components to intraflagellar transport. *Dev Cell* 2012; **22**(5):940–951.
35. Pazour GJ, Baker SA, Deane JA, Cole DG, Dickert BL, Rosenbaum JL, Witman GB, Besharse JC. The intraflagellar transport protein, IFT88, is essential for vertebrate photoreceptor assembly and maintenance. *J Cell Biol* 2002; **157**(1):103–114.
36. Jonassen JA, SanAgustin J, Baker SP, Pazour GJ. Disruption of IFT complex A causes cystic kidneys without mitotic spindle misorientation. *J Am Soc Nephrol* 2012; **23**(4):641–651.
37. Zhang Z, Kostetskii I, Tang W, Haig-Ladewig L, Sapiro R, Wei Z, Patel AM, Bennett J, Gerton GL, Moss SB, Radice GL, Strauss JF, 3rd. Deficiency of SPAG16L causes male infertility associated with impaired sperm motility. *Biol Reprod* 2006; **74**(4):751–759.
38. McDonald K. Osmium ferricyanide fixation improves microfilament preservation and membrane visualization in a variety of animal cell types. *J Ultrastruct Res* 1984; **86**(2):107–118.
39. Meistrich ML, Hess RA. Assessment of spermatogenesis through staging of seminiferous tubules. *Methods Mol Biol* 2013; **927**:299–307.
40. Berruti G, Paiardi C. Acrosome biogenesis: Revisiting old questions to yield new insights. *Spermatogenesis* 2011; **1**(2):95–98.
41. Hartree EF. The acrosome-lysosome relationship. *Reproduction* 1975; **44**(1):125–126.
42. Tang XM, Lalli MF, Clermont Y. A cytochemical study of the Golgi apparatus of the spermatid during spermiogenesis in the rat. *Am J Anat* 1982; **163**(4):283–294.
43. Tang N, Marshall WF. Centrosome positioning in vertebrate development. *J Cell Sci* 2012; **125**(21):4951–4961.

44. Breslow DK, Holland AJ. Mechanism and regulation of centriole and cilium biogenesis. *Annu Rev Biochem* 2019; **88**:11.1–11.34.
45. Iomini C, Babaev-Khaimov V, Sassaroli M, Piperno G. Protein particles in Chlamydomonas flagella undergo a transport cycle consisting of four phases. *J Cell Biol* 2001; **153**(1):13–24.
46. Esparza JM, O'Toole E, Li L, Giddings TH, Jr, Kozak B, Albee AJ, Dutcher SK. Katanin localization requires triplet microtubules in Chlamydomonas reinhardtii. *PLoS One* 2013; **8**(1):e53940.
47. Yamashita YM, Jones DL, Fuller MT. Orientation of asymmetric stem cell division by the APC tumor suppressor and centrosome. *Science* 2003; **301**(5639):1547–1550.
48. Wren KN, Craft JM, Tritschler D, Schauer A, Patel DK, Smith EF, Porter ME, Kner P, Lechtreck KF. A differential cargo-loading model of ciliary length regulation by IFT. *Curr Biol* 2013; **23**(24):2463–2471.
49. Craft JM, Harris JA, Hyman S, Kner P, Lechtreck KF. Tubulin transport by IFT is upregulated during ciliary growth by a cilium-autonomous mechanism. *J Cell Biol* 2015; **208**(2):223–237.
50. Pedersen LB, Miller MS, Geimer S, Leitch JM, Rosenbaum JL, Cole DG. Chlamydomonas IFT172 is encoded by FLA11, interacts with CrEB1, and regulates IFT at the flagellar tip. *Curr Biol* 2005; **15**(3):262–266.
51. Richey EA, Qin H. Dissecting the sequential assembly and localization of intraflagellar transport particle complex B in Chlamydomonas. *PLoS One* 2012; **7**(8):e43118.
52. Iomini C, Li L, Esparza JM, Dutcher SK. Retrograde intraflagellar transport mutants identify complex A proteins with multiple genetic interactions in Chlamydomonas reinhardtii. *Genetics* 2009; **183**(3):885–896.
53. Bhogaraju S, Taschner M, Morawetz M, Basquin C, Lorentzen E. Crystal structure of the intraflagellar transport complex 25/27. *EMBO J* 2011; **30**(10):1907–1918.
54. Johnson LR, Foster JA, Haig-Ladewig L, VanScoy H, Rubin CS, Moss SB, Gerton GL. Assembly of AKAP82, a protein kinase A anchor protein, into the fibrous sheath of mouse sperm. *Dev Biol* 1997; **192**(2):340–350.
55. Turner RM, Eriksson RL, Gerton GL, Moss SB. Relationship between sperm motility and the processing and tyrosine phosphorylation of two human sperm fibrous sheath proteins, pro-hAKAP82 and hAKAP82. *Mol Hum Reprod* 1999; **5**(9):816–824.
56. Miki K, Willis WD, Brown PR, Goulding EH, Fulcher KD, Eddy EM. Targeted disruption of the Akap4 gene causes defects in sperm flagellum and motility. *Dev Biol* 2002; **248**(2):331–342.